Entropy of Surface EMG Reflects Object Weight in Grasp-and-Lift Task*

Yuqi Li[1], Beth Jelfs[1,2] and Rosa H.M. Chan[1,2]

Abstract— **Fingertip force coordination is crucial to the success of grasp-and-lift tasks. In the development of motor prosthesis for daily applications, the ability to accurately classify the desired grasp-and-lift from multi-channel surface electromyography (sEMG) is essential. In order to extract reliable indicators for fingertip force coordination, we searched an extensive set of sEMG features for the optimal subset of relevant features. Using mutual information based feature selection we found that a subset of not more than 10 sEMG features selected from over seven thousand, could effectively classify object weights in grasp-and-lift tasks. Average classification accuracies of 82.53% in the acceleration phase and 88.61% in the isometric contraction phase were achieved. Furthermore, sEMG features associated with object weights and common across individuals were identified. These time-domain features (entropy, mean/median absolute deviation, pNNx) can be calculated efficiently, providing possible new indicators.**

I. INTRODUCTION

Surface electromyography (sEMG) has been extensively utilized in clinical applications and human-machine interfaces [1], [2]. Since the sEMG signal is essentially an aggregate of motor unit action potentials, it reflects both neural activation of muscles and structural changes in the muscle itself [3]. Multi-channel sEMG recorded from several muscles, therefore, provide the ability to estimate both the movements and the force level. Decoding the intention of individuals from sEMG signals is significant in order to provide accurate low-latency control for applications. At the same time, studying the fundamental patterns exhibited by the sEMG when producing different levels of force and during different phases of activation, including acceleration, isometric contraction and relaxation, may shed light on the central nervous system feedback mechanisms that adjust force and torque.

Numerous features in the time and frequency domains have been extracted from sEMG for classification purposes, including amplitude variance, auto-regressive coefficients, median frequency and mean power, to name a few [4]. While, in order to capture the time-frequency characteristics, features have been extracted by wavelet transform and discrete dyadic wavelet transform to achieve accurate recognition [5]. However, a number of factors, such as electrodes placement, can provide uncertainty in sEMG signal collection [6]. Hence, the accuracy of movement identification from sEMG varies across subjects and trials [7]. Thus, the identification of robust features that are minimally entangled with the above factors is desirable.

In this study, we investigated the sEMG data collected from the upper limbs of twelve healthy subjects performing a grasp-and-lift task [8]. Over seven thousand features were extracted from the data, and the features most relevant to the weight of the object were selected using mutual information based algorithms. The selected sEMG features were then used to identify the weight of the object lifted by the individual. Results show it is possible to accurately classify the weight of the objects and that common features can be identified across subjects.

II. DATA AND METHODS

A. The Open-Source sEMG Data

The sEMG data set used in this study is part of the WAY-EEG-GAL database designed to characterize grasp-and-lift tasks [8]. In brief data was collected from twelve right-handed subjects in each trial, the subject was asked to reach for a small object with varying weight (165g, 330g, 660g) and varying surface (silk, suede and sandpaper), grasp it using thumb and index finger, and lift it a few centimeters up in the air, hold it stably for a couple of seconds, and then release the object. From the trials where the object surface was sandpaper, we evaluated the sEMG signals recorded from 5 channels located at the anterior deltoid (DA), brachioradial (BRD), flexor digitorum (FD), common extensor digitorum (CED), and the first dorsal interosseous (FDI) muscles. sEMG data was downsampled to 1kHz before analysis and based on the provided event times we investigated the difference in force related features during the holding and lifting stages described below.

1) Holding Stage: One second of steady-holding was extracted from each trial. During each trial the subject was given an LED cue as to when to begin task and when to release the object. The holding stage time period refers to the last second before the subject was given the signal to release. For each subject, 220 trials were extracted regardless of testing series (weight-varying only, friction-varying only and hybrid series).

2) Lifting Stage: As the subjects lifted the objects at different speeds the duration of the lifting stage varies. For each subject, the time taken from both digits first touching the object to the load force reaching its maximum was

*This work was supported by the Research Grants Council of the Hong Kong Special Administrative Region, China [Project No. CityU110813].

[1]Y. Li, B. Jelfs and R.H.M. Chan are with the Department of Electronic Engineering, City University of Hong Kong, Hong Kong. yuqili3-c@my.cityu.edu.hk, {beth.jelfs,rosachan}@cityu.edu.hk

[2] B. Jelfs and R.H.M. Chan are with the Centre for Biosystems, Neuroscience, and Nanotechnology (CBNN), City University of Hong Kong, Hong Kong.

recorded for each of the same 220 trials as in holding stages. Based on the distribution of these times, the 75th quantile length was fixed as the lifting stage length.

B. Feature Calculation and Normalization

The time-series analysis framework proposed in [9] was used to find possible indicators for the classification of object weight. This framework provides more than one thousand algorithms for univariate time-series analysis spanning a large variety of time-series properties. These properties summarize features of the time-series such as autocorrelation, stationarity, power spectra, information theoretic quantities and many others. Each algorithm, together with predefined parameters, was used to map each sEMG segment to a numerical value. For each segment of the individual sEMG channels, 7778 features were computed. Excluding inapplicable features for each trial, combining all 5 channels, more than 35000 operation values were obtained. To allow the comparison of different operations, the feature values were normalized using z-scoring within a single subject.

C. Feature Selection

Each grasp-and-lift trial was labeled according to the load weight (165g, 330g, 660g). For each subject, there were 220 grasp-and-lift trials, with uneven distribution of load weight (mostly 330g), which were combined to form a matrix of operation values. Two feature selection algorithms were then applied to these operation matrices in order to select the features most relevant to the weight labels. The algorithms chosen for this feature selection problem were both mutual information based algorithms. The Parzen window feature selection (PWFS) [10], concentrates purely on maximizing the mutual information, so can present overfitting within small feature sets. The minimum redundancy maximum relevance (mRMR) feature selection [11] also takes the redundancy within a feature subset into consideration. Combining these two algorithms yields a more stable feature subset. In order to identify possible common features across subjects, 55 trials were drawn randomly from each subject to form an inter-subject model. The same procedure was applied to this inter-subject study.

D. Classification

To deal with imbalanced class distribution (with approximate proportion of 1.23:1.63:1), a 3-class class-weighted linear Support Vector Machine (SVM) classifier with a 10-fold cross validation was chosen to classify load weight based on the first 10 selected features for individual study or the first 20 for common features. We compared the classification accuracies for the object weights using different sets of top selected features.

III. RESULTS

A. Classification Accuracy

Figure 1 shows the classification accuracies for all 12 subjects for both the holding and lifting stages with increasing size of feature set. For all subjects, within 10 features, the classification accuracy reached its maximum after which overfitting occurred. Table 1 summarizes the highest multi-feature classification accuracy (across both algorithms) and the corresponding size of feature set, for both individual subjects and also for the combined data, for each of the stages. Although the two algorithms extracted different feature sets they yielded similar classification accuracies for a single subject. For the common features selected from all subjects the highest classification accuracy was determined for a maximum feature set size of 20. For the holding stage the inter-subject classification accuracy (68.66%) was lower than that of any single-subject accuracy, while in the lifting stage it exceeded only subject 7's accuracy (62.02% vs 60.26%). As the dynamic range of feature values differed in each individual, a subject-tailored model outperformed this universal model.

TABLE I
CLASSIFICATION ACCURACY FOR LIFTING AND HOLDING STAGES

Subject	Lifting Stage		Holding Stage	
	Accuracy (%)	No. of Features	Accuracy (%)	No. of Features
1	88.43	9	74.57	6
2	74.93	4	98.04	4
3	92.54	5	72.63	5
4	87.84	3	88.34	9
5	79.57	2	88.50	7
6	82.19	6	94.48	4
7	60.26	6	86.78	4
8	90.99	8	82.23	4
9	86.39	4	95.05	10
10	87.10	3	96.02	3
11	66.84	6	88.32	3
12	91.14	6	98.34	4
Mean	**82.35**		**88.61**	
Standard Deviation	**10.24**		**8.59**	
Model with Common Features	*62.02*	*5*	*68.66*	*13*

B. Key Features

Table 2 presents a summary of the features and corresponding muscle channels which individually provide the greatest classification accuracy. As both feature selection algorithms have the same initial step, maximizing the mutual information to the class labels, they therefore select the same first feature. For both the lifting and holding stages, the first selected features for each subject, were primarily taken from the brachioradialis. This result implies that during a grasp-and-lift task, more information is gained from the brachioradialis sEMG when compared to the sEMG obtained from the other related muscles. For the single-subject features, entropy, mean/median absolute deviation and pNNx measure all frequently appeared across subjects. The top inter-subject feature selected for both lifting and holding stages was again entropy, which implied feature-universality across subjects.

1) Entropy: Entropy has been used to quantify signal unpredictability in clinical applications [12]. For a continuous

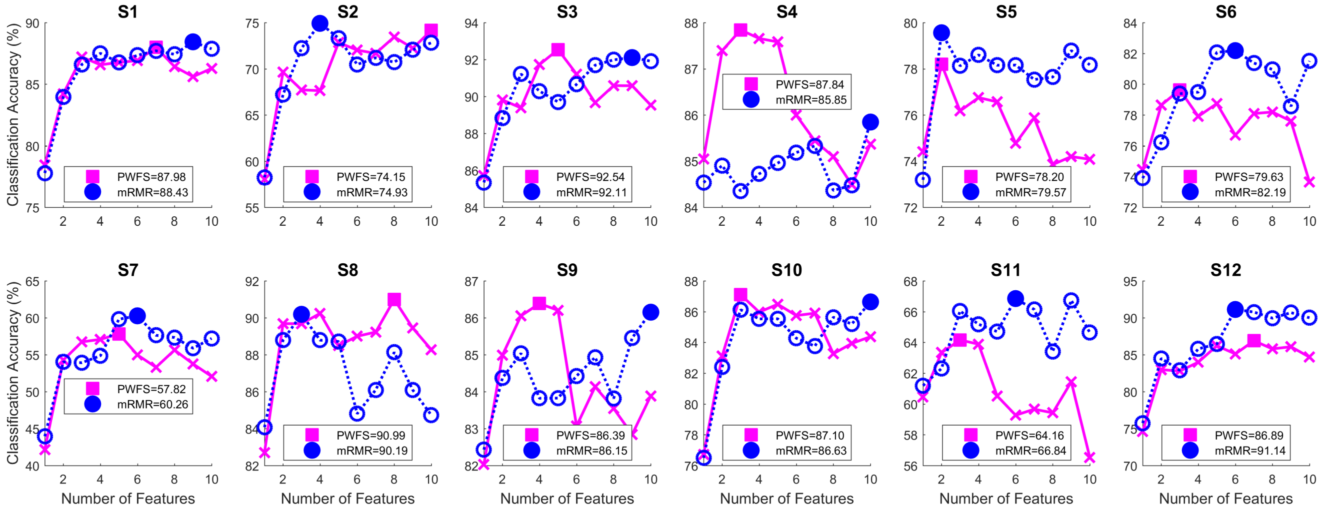

(a) Lifting Stage

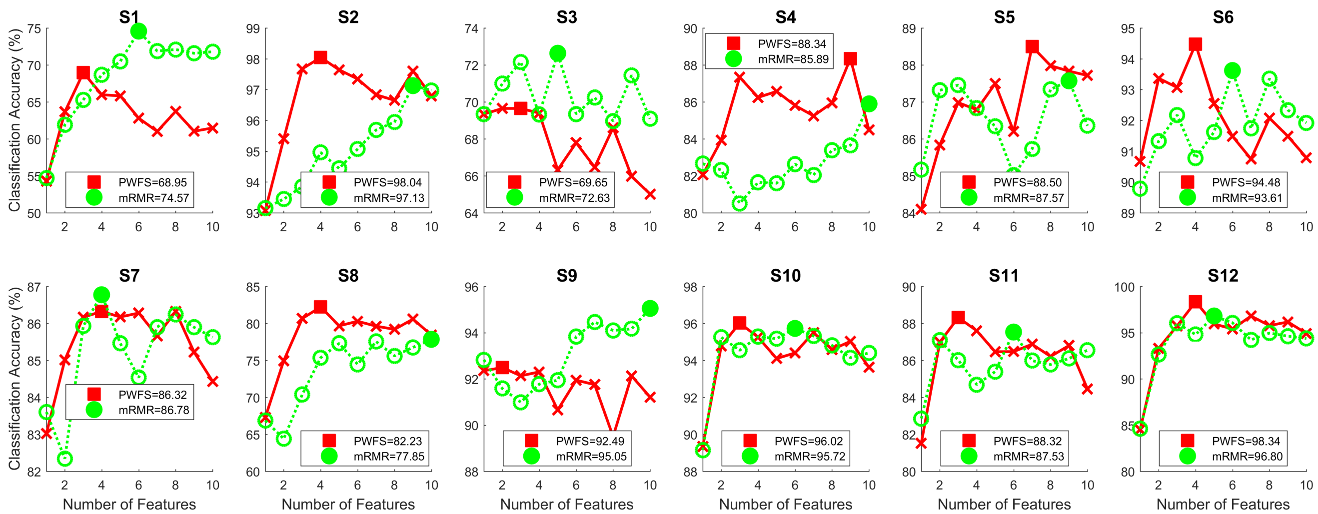

(b) Holding Stage

Fig. 1. Classification accuracies of 12 subjects in (a) lifting stage and (b) holding stage. Solid circle and square stands for the highest classification accuracies in both feature selection algorithms. PWFS: Parzen window feature selection. mRMR: minimum-redundancy-maximum-relevance feature selection.

random variable X, with probability density function $f(x)$, the entropy $H(X)$ is defined as follows:

$$H(X) = -\int_X f(x) \log f(x) \mathrm{d}x \tag{1}$$

However, for a segment of time series with limited sample points, we cannot derive an exact probability density function. Hence, kernel smoothing was used to estimate the probability density function [13]. This estimation, $\hat{f}$, is based on a normal kernel function, and is evaluated at 100 equally-spaced points x_i, that cover the range of the sampled data. The entropy was then computed, with a staircase approximation:

$$H(X) = -\sum_{i=1}^{100} \hat{f}(x_i) \log(\hat{f}(x_i) \times (x_{i+1} - x_i))) \tag{2}$$

Other entropy-based measures of sEMG irregularity such as sample entropy and fuzzy approximate entropy have been shown to correlate with the number of motor units recruited in human upper limbs [14]. However, for the first time, our results reveal that entropy performs better in terms of characterizing the muscle activities in force manipulations than other such complexity based measures.

2) Mean/Median Absolute Deviation: Mean absolute deviation for a N-points time series is computed as follows:

$$\mathrm{MAD} = \frac{1}{N} \sum_{i=1}^{N} |x_i - \bar{x}| \tag{3}$$

and median absolute deviation takes the median value of $|x_i - \bar{x}|$. Both the mean and median absolute deviations provide measures of the dispersion of the data. Similar

TABLE II

TOP FEATURE SELECTED IN LIFTING AND HOLDING STAGES AND THE CORRESPONDING CLASSIFICATION ACCURACY USING THIS SINGLE FEATURE

Subject	Lifting Stage		Holding Stage	
	(Muscle) Name of the Top Feature	Accuracy (%)	(Muscle) Name of the Top Feature	Accuracy (%)
1	(BRD) pNN30	78.44	(FDI) Autoregressive Model (Covariance)	54.26
2	(FDI) Interquartile Range	58.05	(FDI) Entropy	93.07
3	(BRD) Entropy	85.71	(BRD) Median Absolute Deviation	69.34
4	(BRD) Entropy	85.05	(BRD) Entropy	82.06
5	(BRD) pNN20	74.41	(BRD) Entropy	84.10
6	(BRD) Mean Absolute Deviation	74.44	(BRD) Mean Absolute Deviation	90.67
7	(BRD) Mean Absolute Deviation	42.17	(BRD) pNN20	83.02
8	(BRD) Entropy	82.70	(BRD) Entropy	67.26
9	(BRD) Interquartile Range	82.03	(BRD) Heart Rate Variability Measure	92.35
10	(BRD) pNN20	76.71	(BRD) Entropy	89.33
11	(BRD) Mean Absolute Deviation	60.45	(BRD) Heart Rate Variability Measure	81.52
12	(FDI) Compare Kernel Smoothings Fitness	74.62	(BRD) Entropy	84.50
Model with Common Feature	*(BRD) Entropy*	*54.82*	*(BRD) Entropy*	*55.91*

Each feature was labeled according to the sEMG channel. Format: (Muscle)Feature. Muscle acronyms {BRD: Brachioradialis. FDI: First Dorsal Interosseous.}

measures of sEMG dispersion, such as variance, have been extensively used in sEMG analysis [4].

3) pNNx Measure: The pNNx family of measures was originally proposed to examine cycle length variability in the time domain [15]. Here x is a threshold to indicate the irregularity and this parameter usually ranges from 10 to 100. When dealing with a N-points time series y, the pNNx value is computed as follows:

$$\begin{gathered} z_i = (y_{i+1} - y_i) \times 1000, \quad i = 1, \ldots, N-1 \\ \text{pNNx} = \frac{\text{Number of } z_i > x}{N-1} \end{gathered} \tag{4}$$

The sequence z_i represents the amplitude change under a certain sampling frequency. The pNNx measure evaluates the fraction of positive changes that are above different thresholds x.

IV. CONCLUSION

In this study we effectively classified the object weight in a grasp-and-lift task with less than ten sEMG features. Using two mutual-information based feature selection methods subject-tailored feature vectors were obtained from 7778 features. On average, we achieved $82.35 \pm 10.24\%$ and $88.61 \pm 8.59\%$ (Mean±Standard Deviation) classification accuracy during acceleration and isometric contraction phase, respectively. We found that in both phases, some features common across individuals, in particular entropy, correlate with the weight of the object being lifted by all individuals. These features may be able to provide more accurate clinical indicators, such as muscle assessment in rehabilitation engineering. But the possible physiological relation between force levels and these features of sEMG requires further investigation, for instance, simulations of muscle fibers and muscle structure.

ACKNOWLEDGMENT

The authors would like to thank Dr. Xiaoling Hu for the valuable discussion on feature interpretation.

REFERENCES

[1] M. R. Ahsan, M. I. Ibrahimy, O. O. Khalifa, *et al.*, "EMG signal classification for human computer interaction: a review," *Eur. J. Sci. Res.*, vol. 33, no. 3, pp. 480–501, 2009.

[2] C. Frigo and P. Crenna, "Multichannel sEMG in clinical gait analysis: a review and state-of-the-art," *Clin. Biomech.*, vol. 24, no. 3, pp. 236–245, 2009.

[3] J. Basmajian and C. De Luca, *Muscles Alive: Their Functions Revealed by Electromyography*. Williams & Wilkins, 1985.

[4] A. Phinyomark, P. Phukpattaranont, and C. Limsakul, "Feature reduction and selection for EMG signal classification," *Expert Syst. Appl.*, vol. 39, no. 8, pp. 7420–7431, 2012.

[5] M.-F. Lucas, A. Gaufriau, S. Pascual, C. Doncarli, and D. Farina, "Multi-channel surface EMG classification using support vector machines and signal-based wavelet optimization," *Biomed. Signal Process. Control*, vol. 3, no. 2, pp. 169–174, 2008.

[6] D. Farina, R. Merletti, and R. M. Enoka, "The extraction of neural strategies from the surface EMG," *J. Appl. Physiol.*, vol. 96, no. 4, pp. 1486–1495, 2004.

[7] X. Zhai, B. Jelfs, R. H. M. Chan, and C. Tin, "Short latency hand movement classification based on surface EMG spectrogram with PCA," in *International Conference of the IEEE Engineering in Medicine and Biology Society (EMBC)*, 2016, pp. 327–330.

[8] M. D. Luciw, E. Jarocka, and B. B. Edin, "Multi-channel eeg recordings during 3,936 grasp and lift trials with varying weight and friction," *Sci. Data*, vol. 1, p. 140047, 2014.

[9] B. D. Fulcher, M. A. Little, and N. S. Jones, "Highly comparative time-series analysis: the empirical structure of time series and their methods," *J. R. Soc. Interface*, vol. 10, no. 83, p. 20130048, 2013.

[10] N. Kwak and C.-H. Choi, "Input feature selection by mutual information based on parzen window," *IEEE Trans. Pattern Anal. Mach. Intell.*, vol. 24, no. 12, pp. 1667–1671, 2002.

[11] H. Peng, F. Long, and C. Ding, "Feature selection based on mutual information criteria of max-dependency, max-relevance, and min-redundancy," *IEEE Trans. Pattern Anal. Mach. Intell.*, vol. 27, no. 8, pp. 1226–1238, 2005.

[12] M. Sabeti, S. Katebi, and R. Boostani, "Entropy and complexity measures for EEG signal classification of schizophrenic and control participants," *Artif. Intell. Med.*, vol. 47, no. 3, pp. 263–274, 2009.

[13] M. P. Wand and M. C. Jones, *Kernel smoothing*. CRC Press, 1994.

[14] D. Ao, R. Sun, K.-y. Tong, and R. Song, "Characterization of stroke- and aging-related changes in the complexity of EMG signals during tracking tasks," *Ann. Biomed. Eng.*, vol. 43, no. 4, pp. 990–1002, 2015.

[15] J. Mietus, C. Peng, I. Henry, R. Goldsmith, and A. Goldberger, "The pNNx files: re-examining a widely used heart rate variability measure," *Heart*, vol. 88, no. 4, pp. 378–380, 2002.